

# Stochastic oscillations in models of epidemics on a network of cities

G. Rozhnova<sup>1</sup>, A. Nunes<sup>1</sup> and A. J. McKane<sup>1,2</sup>

<sup>1</sup>*Centro de Física da Matéria Condensada and Departamento de Física,  
Faculdade de Ciências da Universidade de Lisboa, P-1649-003 Lisboa Codex, Portugal*

<sup>2</sup>*Theoretical Physics Division, School of Physics and Astronomy,  
University of Manchester, Manchester M13 9PL, United Kingdom*

We carry out an analytic investigation of stochastic oscillations in a susceptible-infected-recovered model of disease spread on a network of  $n$  cities. In the model a fraction  $f_{jk}$  of individuals from city  $k$  commute to city  $j$ , where they may infect, or be infected by, others. Starting from a continuous time Markov description of the model the deterministic equations, which are valid in the limit when the population of each city is infinite, are recovered. The stochastic fluctuations about the fixed point of these equations are derived by use of the van Kampen system-size expansion. The fixed point structure of the deterministic equations is remarkably simple: a unique non-trivial fixed point always exists and has the feature that the fraction of susceptible, infected and recovered individuals is the same for each city irrespective of its size. We find that the stochastic fluctuations have an analogously simple dynamics: all oscillations have a single frequency, equal to that found in the one city case. We interpret this phenomenon in terms of the properties of the spectrum of the matrix of the linear approximation of the deterministic equations at the fixed point.

PACS numbers: 05.40.-a, 87.10.Mn, 02.50.Ey

## I. INTRODUCTION

Two of the ideas that are currently dominating the discussion of modeling epidemic spread are those of stochasticity and network structure [1–6]. Deterministic models of the Susceptible-Infected-Recovered (SIR) type have a long history [7, 8] and have been thoroughly investigated [9, 10] along with many extensions of the models such as age classes or higher-order nonlinear interaction terms. Although stochasticity, due to random processes at the level of individuals, and networks, either between individuals or towns and cities, were recognised early on as significant and important factors, the tendency was to model them through computer simulations. This is not surprising: it is rather straightforward to deal with stochastic behavior in simulations, and similarly the analytic methods available to investigate complex networks, especially adaptive networks, are limited. There has also been a tendency towards developing extremely detailed agent-based models to study disease spread [11–14], which are the antithesis of the simple analytic approach based on the original SIR deterministic model.

In parallel with these developments, however, there have been several efforts to extend analytic studies into the realm of stochastic and network dynamics. The SIR model can be formulated as an individual-based model (IBM) which can form a starting point for both an analytical treatment, based on the master equation (continuous-time Markov chain) [15, 16], and numerical simulations, based on the Gillespie algorithm [17]. The analytical studies use the system-size expansion of van Kampen to reduce the master equation to the set of deterministic equations previously studied, together with a set of stochastic differential equations for the deviations from the deterministic result. As long as one is not too close to the fade-out boundary, there is no need to go be-

yond next-to-leading order in the expansion parameter,  $1/\sqrt{N}$ , where  $N$  is the number of individuals in the system. This already gives results which are, in general, in almost perfect agreement with the results of simulations [18, 19].

This approach has been used to study the stochastic version of the standard SIR model [19], the Susceptible-Exposed-Infected-Recovered (SEIR) model [20], both these models with annual forcing [20, 21], staged-models [22, 23], the pair-approximation in networked models [24, 25], amongst others. In this paper we extend the treatment to a metapopulation model for disease spread, which consists of  $n$  cities (labeled  $j = 1, \dots, n$ ), each of which contains  $N_j$  individuals. A fraction of the population of city  $k$ ,  $f_{jk}$ , commutes to city  $j$  and this defines the strength of the link from node  $k$  to  $j$  in the network of cities. We will show that the methods used in the case of one city carry over to the case where the system comprises of a network of cities, and that a surprisingly simple set of results can be derived which allow us to make quite general predictions for a class of stochastic networked models of epidemics.

The starting point for our analysis is a specification of how commuters move between cities in the network. As will become clear, the model we arrive at will not depend on the details of how and when these exchanges take place. We then write down transition rates for the usual SIR process, now taking account the city of origin of the infector and infected individuals. From the resulting equation we can immediately find the deterministic equations corresponding to the stochastic model when  $N_j \rightarrow \infty$  for all  $j$ . Deterministic models of this type began to be considered long ago [26] and the existence and stability properties of the endemic equilibrium were studied for different formulations of the coupling between the cities and of the disease dynamics [27–29]. Stochastic

effects in these systems have also been analyzed from the point of view of the relation between spatial heterogeneity, disease extinction and the threshold for disease onset [27, 30–32].

Some rather strong and general results on the uniqueness and global stability of the fixed points of the deterministic model are known [33]. We will use these results and then go beyond this leading-order analysis to determine the linear stochastic corrections that characterize the quasi-stationary state of the finite system. As expected, the qualitative predictions of the deterministic model are shown to be incorrect; instead large stochastic cycles are found, although their form is much simpler than might naively have been expected. We show that this is, in part, a reflection of the special nature of the fixed points of the deterministic model.

The outline of the paper is as follows. In Section II we describe the basic model and apply it to the case of two cities. The generalization to the  $n$ -city case is given in Section III. The results for the form of the sustained oscillations are given in Section IV and we conclude in Section V. Two appendices contain technical details which are too cumbersome to include in the main text.

## II. TWO-CITY MODEL

In this section we will formulate the model when there are only two cities; the general  $n$  city case described in Section III does not introduce any new points of principle and is easily explained once the two city case has been understood.

The SIR model consists of three classes of individuals: susceptibles, infected and recovered. The number of individuals in the three classes belonging to city  $j$  will be denoted by  $S_j, I_j$  and  $R_j$  respectively. We assume that births and deaths are coupled at the individual level, so that when an individual dies another (susceptible) individual is born. This means that the number of individuals belonging to any one city,  $N_j$ , does not change with time, and so the number of recovered individuals is not an independent variable:  $R_j = N_j - S_j - I_j$ , where  $j = 1, 2$  [19].

There are four processes in the SIR model which cause transitions to a new state: infection, recovery, death of an infected individual and death of a recovered individual. The death of a susceptible individual does not cause a transition, since it is immediately replaced by another, newborn, individual which is by definition susceptible. Of the four listed processes, the final three only involve one individual and so only involve one city. The transition rates are [19]:

- (a) Recovery of an infective individual (and creation of a recovered individual)

$$\begin{aligned} T_1 &\equiv T(S_1, I_1 - 1, S_2, I_2 | S_1, I_1, S_2, I_2) = \gamma I_1, \\ T_2 &\equiv T(S_1, I_1, S_2, I_2 - 1 | S_1, I_1, S_2, I_2) = \gamma I_2. \end{aligned} \quad (1)$$

- (b) Death of an infected individual (and birth of a susceptible individual):

$$\begin{aligned} T_3 &\equiv T(S_1 + 1, I_1 - 1, S_2, I_2 | S_1, I_1, S_2, I_2) = \mu I_1, \\ T_4 &\equiv T(S_1, I_1, S_2 + 1, I_2 - 1 | S_1, I_1, S_2, I_2) = \mu I_2. \end{aligned} \quad (2)$$

- (c) Death of a recovered individual (and birth of a susceptible individual):

$$\begin{aligned} T_5 &\equiv T(S_1 + 1, I_1, S_2, I_2 | S_1, I_1, S_2, I_2) = \mu(N_1 - S_1 - I_1), \\ T_6 &\equiv T(S_1, I_1, S_2 + 1, I_2 | S_1, I_1, S_2, I_2) = \mu(N_2 - S_2 - I_2). \end{aligned} \quad (3)$$

Here  $\gamma$  and  $\mu$  are parameters which respectively characterize the rate of recovery and of birth/death.

The infection processes introduce the role of the commuters. We let  $f_{21}$  be the fraction of the population from city 1 which commutes to city 2, leaving a fraction  $(1 - f_{21})$  of the population as residents of city 1. Similarly, for commuters from city 2, as illustrated in Fig. 1. We note that the number of individuals in city  $j$  is  $M_j = (1 - f_{kj})N_j + f_{jk}N_k$ , where  $j \neq k$ . We will not specify the nature of the commute in more detail and assume that the  $f_{jk}$  are a property of the corresponding pair of cities that defines the overall average fraction of time that an individual from one city spends in the other city. These coefficients will be taken as a coarse-grained measure of the demographic coupling between the cities that will be applied to all individuals independently of disease status and do not discriminate between different types of stays with their typical frequencies and durations.

To see the nature of the infective interactions that occur, we first fix our attention on those involving susceptible individuals from city 1. There are four types of term:

- (i) Infective residents in city 1 infect susceptible residents in city 1.
- (ii) Infective commuters from city 2 infect susceptible residents in city 1.
- (iii) Infective residents in city 2 infect susceptible commuters from city 1.
- (iv) Infective commuters from city 1 infect susceptible commuters from city 1 in city 2.

The rates for these to occur according to the usual prescription for the SIR model [19] are:

- (i)  $\beta (1 - f_{21}) S_1 (1 - f_{21}) I_1 / M_1$ ,
- (ii)  $\beta (1 - f_{21}) S_1 f_{12} I_2 / M_1$ ,
- (iii)  $\beta f_{21} S_1 (1 - f_{12}) I_2 / M_2$ ,
- (iv)  $\beta f_{21} S_1 f_{21} I_1 / M_2$ ,

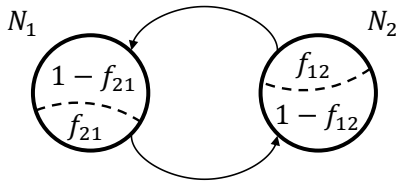


FIG. 1: A fraction  $f_{jk}$  of residents of city  $k$  commute to city  $j$ , where  $j, k = 1, 2$ .

where  $\beta$  is the parameter which sets the overall rate of infection. Adding these rates together we obtain the total transition rate for infection of  $S_1$  individuals as

$$\beta \left[ c_{11} \frac{S_1 I_1}{N_1} + c_{12} \frac{S_1 I_2}{N_2} \right],$$

where

$$c_{11} = \frac{(1-f_{21})^2 N_1}{M_1} + \frac{f_{21}^2 N_1}{M_2},$$

$$c_{12} = \frac{(1-f_{21}) f_{12} N_2}{M_1} + \frac{f_{21} (1-f_{12}) N_2}{M_2}.$$

A similar analysis can be made for the transitions involving susceptible individuals from city 2. Putting these results together we obtain the transition rates for infection as

(d) Infection of a susceptible individual:

$$T_7 \equiv T(S_1 - 1, I_1 + 1, S_2, I_2 | S_1, I_1, S_2, I_2)$$

$$= \beta \left[ c_{11} \frac{S_1 I_1}{N_1} + c_{12} \frac{S_1 I_2}{N_2} \right],$$

$$T_8 \equiv T(S_1, I_1, S_2 - 1, I_2 + 1 | S_1, I_1, S_2, I_2)$$

$$= \beta \left[ c_{21} \frac{S_2 I_1}{N_1} + c_{22} \frac{S_2 I_2}{N_2} \right], \quad (4)$$

where

$$c_{11} = \frac{(1-f_{21})^2}{1-f_{21}+f_{12}q} + \frac{f_{21}^2}{f_{21}+(1-f_{12})q},$$

$$c_{12} = \frac{(1-f_{21})f_{12}q}{1-f_{21}+f_{12}q} + \frac{f_{21}(1-f_{12})q}{f_{21}+(1-f_{12})q},$$

$$c_{21} = \frac{(1-f_{12})f_{21}}{f_{21}+(1-f_{12})q} + \frac{f_{12}(1-f_{21})}{1-f_{21}+f_{12}q},$$

$$c_{22} = \frac{(1-f_{12})^2 q}{f_{21}+(1-f_{12})q} + \frac{f_{12}^2 q}{1-f_{21}+f_{12}q}, \quad (5)$$

and  $q = N_2/N_1$ . We assume that  $N_1$  and  $N_2$  are not too different, so that  $q$  is neither very small nor very large.

The model is defined by the transitions rates in Eqs. (1)-(4). It is interesting that the transitions due to infection depend on the fractions  $f_{jk}$  only through the

constants  $c_{jk}$  defined in Eq. (5). Other ways of accounting for commuting individuals would typically still give rise to the form given in Eq. (4), but with the constants  $c_{jk}$  defined in a different way.

Since our counting of the ways that infection takes place was exhaustive, we expect that the constants  $c_{jk}$  are not independent. It is straightforward to check that they obey the following relations:

$$c_{11} + c_{12} = 1, \quad c_{21} + c_{22} = 1, \quad c_{12} = c_{21}q. \quad (6)$$

So there are only two independent parameters in addition to the usual SIR parameters  $\beta, \gamma$  and  $\mu$  found in the single city case, and we choose these to be  $c_{12}$  and  $q = N_2/N_1$ . Our results will be given in terms of these two parameters. It is easy to see that, for each  $q$ , the range of  $c_{12}$  is the interval  $[0, q/(q+1)]$  where the maximum is attained for  $f_{21} + f_{12} = 1$ . While exploring the general behavior of the system we will consider the  $c_{jk}$  independently of the underlying microscopic model as positive parameters that take values in the wider admissible range defined by the constraints (6).

Having specified the model it may be investigated in two ways as indicated in Section I. First, it can be simulated with Gillespie's algorithm [17], or some equivalent method. Second, it can be studied analytically by constructing the master equation and performing van Kampen's system size expansion on this equation. This will be the main focus of this paper. For notational convenience we will denote the states of the system by  $\sigma \equiv \{S_1, I_1, S_2, I_2\}$ , recalling that the number of recovered individuals from each city may be written in terms of these variables. The master equation gives the time evolution of  $P(\sigma, t)$ , the probability distribution for finding the system in state  $\sigma$  at time  $t$ . It takes the form [15, 16]

$$\frac{dP(\sigma, t)}{dt} = \sum_{\sigma' \neq \sigma} \sum_{a=1}^8 [T_a(\sigma|\sigma')P(\sigma', t) - T_a(\sigma'|\sigma)P(\sigma, t)], \quad (7)$$

where  $T_a(\sigma|\sigma')$ ,  $a = 1, \dots, 8$  are the transition rates from the state  $\sigma'$  to the state  $\sigma$  given explicitly in Eqs. (1)-(4).

The full master equation (7) cannot be solved, but the van Kampen system-size expansion when taken to next-to-leading order usually gives results which are in excellent agreement with simulations. We will see that this will also be the case in the extensions of the method which we are exploring in this paper. The system-size expansion starts by making the following ansatz [15]:

$$S_j = N_j s_j + N_j^{1/2} x_j, \quad I_j = N_j i_j + N_j^{1/2} y_j, \quad (8)$$

where  $j = 1, 2$ . Here  $s_j = \lim_{N_j \rightarrow \infty} S_j/N_j$  and  $i_j = \lim_{N_j \rightarrow \infty} I_j/N_j$  are the fraction of individuals from city  $j$  which are respectively susceptible and infected in the deterministic limit. The quantities  $x_j$  and  $y_j$  are the stochastic deviations from these deterministic results, suitably scaled so that they also become continuous in

the limit of large population sizes. The ansatz (8) is substituted into Eq. (7) and powers of  $\sqrt{N_j}$  on the left- and right-hand sides matched up. The leading order contribution gives the deterministic equations of the model and the next-to-leading order linear stochastic differential equations for  $x_j$  and  $y_j$ . We shall not describe the method in great detail, since it is described clearly in van Kampen's book [15] and in many papers, including several on the SIR model [6, 19, 22]. Instead we will outline the main results of the approximation in the remainder of this section, and give some explicit intermediate formulas in Appendix A.

The deterministic equations which are found to first order in the system-size expansion can also be obtained by multiplying Eq. (7) by  $S_1, I_1, S_2$  and  $I_2$  in turn and then summing over all states  $\sigma$ . This yields

$$\begin{aligned}\frac{ds_1}{dt} &= -\beta s_1 (c_{11}i_1 + c_{12}i_2) + \mu(1 - s_1), \\ \frac{ds_2}{dt} &= -\beta s_2 (c_{21}i_1 + c_{22}i_2) + \mu(1 - s_2), \\ \frac{di_1}{dt} &= \beta s_1 (c_{11}i_1 + c_{12}i_2) - (\gamma + \mu)i_1, \\ \frac{di_2}{dt} &= \beta s_2 (c_{21}i_1 + c_{22}i_2) - (\gamma + \mu)i_2.\end{aligned}\quad (9)$$

For the case of cities with equal population sizes, these have been previously found and analyzed in [28]. In the context of the present work we are mainly interested in the fixed points of these equations. We will not discuss these here, instead we will wait until Section III, where the case of  $n$  cities will be discussed when we can give a more general treatment.

Of more interest to us in this paper are the variables  $x_j$  and  $y_j$  which describe the linear fluctuations around trajectories of the deterministic set of equations (9). For convenience we will introduce the vector of these fluctuations  $\mathbf{z} = (x_1, x_2, y_1, y_2)$ . Our focus will be on fluctuations in the stationary state, that is, about the non-trivial fixed point of the deterministic equations (which we will show in the next section is unique). The fluctuations obtained through the system-size expansion obey a linear Fokker-Planck equation, which is equivalent to a set of stochastic differential equations of the form [16]

$$\frac{dz_J}{dt} = \sum_{K=1}^4 A_{JK} z_K + \eta_J(t), \quad J = 1, \dots, 4, \quad (10)$$

where  $\eta_J(t)$  are Gaussian noise terms with zero mean which satisfy  $\langle \eta_J(t) \eta_K(t') \rangle = B_{JK} \delta(t - t')$ . Since the fluctuations are about the fixed point, the  $4 \times 4$  matrices  $A$  and  $B$  are independent of time, and completely characterize the fluctuations. They are given explicitly in Appendix A.

The fluctuations will be analyzed in detail in Section IV, when they will also be compared to the results of numerical simulations. Before discussing this, we will generalize the discussion of this section to an arbitrary network of  $n$  cities.

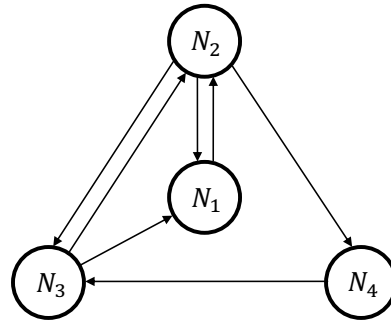


FIG. 2: Individuals commute between  $n$  cities, illustrated for a particular network when  $n = 4$ .

### III. ARBITRARY NETWORK STRUCTURE

In this section we will generalize the content of Section II to  $n$  cities and also find the fixed points of the deterministic dynamics in this case.

#### A. $n$ -city model

We use the same notation as in Section II, labeling the cities by  $j$  and  $k$  which now run from 1 to  $n$ . It will be convenient to introduce the quantity

$$f_j = \sum_{k \neq j} f_{kj}, \quad (11)$$

so that the number of individuals in city  $j$  may be written as

$$\begin{aligned}M_j &= \left[1 - \sum_{k \neq j} f_{kj}\right] N_j + \sum_{k \neq j} f_{jk} N_k \\ &= (1 - f_j) N_j + \sum_{k \neq j} f_{jk} N_k.\end{aligned}\quad (12)$$

There are, once again, four types of term in the process of infection (see Figure 2) and we again fix our attention on those involving susceptible individuals from city 1:

- (i) Infective residents in city 1 infect susceptible residents in city 1. This gives a rate of  $\beta(1 - f_1)S_1(1 - f_1)I_1/M_1$ .
- (ii) Infective commuters from city  $j$ ,  $j = 2, \dots, n$ , infect susceptible residents in city 1. This gives a rate, summing over all  $j$ , of  $\beta(1 - f_1)S_1 \sum_{j \neq 1} f_{j1}I_j/M_1$ .
- (iii) Infective residents in city  $j$ ,  $j = 2, \dots, n$ , infect susceptible commuters from city 1. This gives a rate, summing over all  $j$ , of  $\beta \sum_{j \neq 1} (1 - f_j)I_j f_{j1}S_1/M_j$ .
- (iv) Infective commuters from city  $k$  (including city 1) infect susceptible commuters from city 1 in city  $j$ . This gives a total rate of  $\beta \sum_{j \neq 1} f_{j1}S_1 \sum_{k \neq j} f_{jk}I_k/M_j$ .

Since the transition rates for recovery and birth/death are simple extensions of those for two cities we can now write down the transition rates for the  $n$ -city model as:

- (a) Recovery of an infective individual (and creation of a recovered individual)

$$T_j \equiv T(S_1, I_1, \dots, S_j, I_j - 1, \dots, S_n, I_n | \sigma) = \gamma I_j, \quad (13)$$

- (b) Death of an infected individual (and birth of a susceptible individual):

$$T_{n+j} \equiv T(S_1, I_1, \dots, S_j + 1, I_j - 1, \dots, S_n, I_n | \sigma) = \mu I_j, \quad (14)$$

- (c) Death of a recovered individual (and birth of a susceptible individual):

$$\begin{aligned} T_{2n+j} &\equiv T(S_1, I_1, \dots, S_j + 1, I_j \dots, S_n, I_n | \sigma) \\ &= \mu(N_j - S_j - I_j), \end{aligned} \quad (15)$$

- (d) Infection of a susceptible individual:

$$\begin{aligned} T_{3n+j} &\equiv T(S_1, I_1, \dots, S_j - 1, I_j + 1 \dots, S_n, I_n | \sigma) \\ &= \beta \sum_{k=1}^n c_{jk} \frac{S_j I_k}{N_k}, \end{aligned} \quad (16)$$

where  $\sigma \equiv \{S_1, I_1, \dots, S_j, I_j \dots, S_n, I_n\}$  and where  $j = 1, \dots, n$ . The coefficients  $c_{jk}$  in Eq. (16) may be read off from the terms (i)-(iv), but they are sufficiently complicated to write down in full that we only list them in Appendix B. In that Appendix we also show that relations between the  $c_{jk}$ , analogous to those given in Eq. (6) for the two-city case hold, and are given by

$$c_{jj} + \sum_{k \neq j} c_{jk} = 1; \quad c_{kj} = \left( \frac{N_j}{N_k} \right) c_{jk}; \quad j, k = 1, \dots, n. \quad (17)$$

So in the  $n$ -city model, there are  $n(n-1)/2$  independent coupling parameters  $c_{jk}$  and  $(n-1)$  parameters for city sizes in addition to the usual epidemiological parameters. Note that if all city sizes are equal the second relation in Eq. (17) reduces to  $c_{kj} = c_{jk}$ . This symmetry will be used in the subsequent analysis.

Following the same path as in Section II, having specified the model by giving the transition rates, we move on to the dynamics. The process is Markovian and so satisfies the master equation (7) except now the sum on  $a$  goes from 1 to  $4n$ . As detailed in Appendix A, invoking the van Kampen ansatz (8) gives the following deterministic equations to leading order:

$$\begin{aligned} \frac{ds_j}{dt} &= -\beta s_j \sum_{k=1}^n c_{jk} i_k + \mu(1 - s_j), \\ \frac{di_j}{dt} &= \beta s_j \sum_{k=1}^n c_{jk} i_k - (\gamma + \mu) i_j, \end{aligned} \quad (18)$$

where  $j = 1, \dots, n$ . At next-to-leading order the fluctuations are found to satisfy the linear stochastic differential equation (10), but with  $J, K = 1, \dots, 2n$ . The two matrices  $A$  and  $B$  are given explicitly in Appendix A. They are independent of time, since they are evaluated at the fixed points of the dynamics (18). For the rest of this section we will investigate the fixed point structure of these equations.

## B. The fixed points of the deterministic equations

The fixed points of the deterministic equations (18) will be denoted by asterisks. Adding the two sets of equations we immediately see that

$$(\gamma + \mu) i_j^* = \mu(1 - s_j^*), \quad j = 1, \dots, n. \quad (19)$$

Using this equation to eliminate the  $i_j^*$ , and also using Eq. (17), one finds that

$$s_j^* \left[ (\beta + \gamma + \mu) - \beta \sum_{k=1}^n c_{jk} s_k^* \right] = (\gamma + \mu), \quad j = 1, \dots, n. \quad (20)$$

Two fixed points can be found by inspection. First, suppose one of the  $i_j^*$  is zero, for instance  $i_\ell^* = 0$ . Then from Eq. (19)  $s_\ell^* = 1$ . From Eq. (18) we see immediately that  $\sum_{k=1}^n c_{\ell k} i_k^* = 0$ . Since the coefficients  $c_{jk}$  are non-negative (see Appendix B), then  $i_k^* = 0$  for all  $k$  as long as  $c_{\ell k} \neq 0$ . Using the  $i_k^*$  which are zero as input into Eq. (18), in the same way as we did originally for  $i_\ell^*$ , we see that as long as the cities are connected by non-zero  $c_{jk}$ , then they will have no infected individuals present. From Eq. (19) it follows that  $s_k^* = 1$  for these cities. This is the trivial solution where no infection is present anywhere in this cluster of connected cities. We will assume that all the cities are connected either directly or indirectly, so that  $i_k^* = 0, s_k^* = 1$  for all  $k$ .

Of more interest is what we will call ‘‘the symmetric fixed point’’. This has  $s_k^* = s^*$ , a constant, for all  $k$ . From Eq. (19) one sees that the  $i_k^*$  are also independent of  $k$ , and we denote them by  $i^*$ . Using Eq. (17),  $s^*$  and  $i^*$  are found to satisfy the equations

$$\begin{aligned} s^* [(\beta + \gamma + \mu) - \beta s^*] &= (\gamma + \mu), \\ (\gamma + \mu) i^* &= \mu(1 - s^*), \end{aligned} \quad (21)$$

which are the fixed point equations for the ordinary ‘one-city’ SIR model [7, 8]. As is well known these may be solved to give for the non-trivial fixed point

$$s^* = \frac{\gamma + \mu}{\beta}, \quad i^* = \frac{\mu[\beta - (\gamma + \mu)]}{\beta(\gamma + \mu)}. \quad (22)$$

Due to a remarkable theorem, we can assert that the symmetric solution given by Eq. (22) is the only non-trivial fixed point of the deterministic equations (18) [33]. This is proved by finding a Liapunov function for the  $n$ -city SIR model. In fact the result is more general than

we require and was proved for the SEIR model; in Appendix B we give the explicit form of the Liapunov function for the SIR model and a brief outline of the proof following the argument in Ref. [33] for this simpler case. The theorem also tells us that the non-trivial fixed point (22) is globally stable. Therefore we can now go on to study stochastic fluctuations about this well characterized attractor.

#### IV. SPECTRUM OF THE STOCHASTIC FLUCTUATIONS

Based on previous studies of stochastic fluctuations in the SIR model in different contexts, we would expect that the fixed point behavior predicted in the deterministic limit is replaced by large stochastic oscillations [18, 19]. In effect, the noise due to the randomness of the processes in the IBM, sustains the natural tendency for cycles to occur, and amplifies them through a resonance effect. Since the oscillations are stochastic, straightforward averaging will simply wipe out the cyclic structure; to understand the nature of the fluctuations we need to Fourier transform them and then pick out the dominant frequencies.

So we begin by taking the Fourier transform of the linear stochastic differential equation Eq. (10) (generalized to the case of  $n$  cities) to find

$$\sum_{K=1}^{2n} (-i\omega\delta_{JK} - A_{JK}) \tilde{z}_K(\omega) = \tilde{\eta}_J(\omega), \quad J = 1, \dots, 2n, \quad (23)$$

where the  $\tilde{f}$  denotes the Fourier transform of the function  $f$ . Defining the matrix  $-i\omega\delta_{JK} - A_{JK}$  to be  $\Phi_{JK}(\omega)$ , the solution to Eq. (23) is

$$\tilde{z}_J(\omega) = \sum_{K=1}^{2n} \Phi_{JK}^{-1}(\omega) \tilde{\eta}_K(\omega). \quad (24)$$

The power spectrum for fluctuations carrying the index  $J$  is defined by

$$P_J(\omega) \equiv \langle |\tilde{z}_J(\omega)|^2 \rangle = \sum_{K=1}^{2n} \sum_{L=1}^{2n} \Phi_{JK}^{-1}(\omega) B_{KL} (\Phi^\dagger)^{-1}_{LJ}(\omega). \quad (25)$$

Since  $\Phi = -i\omega I - A$ , where  $I$  is the  $2n \times 2n$  unit matrix, and since  $A$  and  $B$  are independent of  $\omega$ , the structure of  $P_J(\omega)$  is that of a polynomial of degree  $4n - 2$  divided by another polynomial of degree  $4n$ . The explicit form of the denominator is  $|\det \Phi(\omega)|^2$ .

Oscillations with well-defined frequencies should show up as peaks in the power-spectrum. The structure of the power spectrum described above — with the ratio of polynomials of high order potentially giving rise to many maxima — might lead us to suppose that the spectrum of fluctuations would have a rather complex structure. In fact numerical simulations indicate that only a single

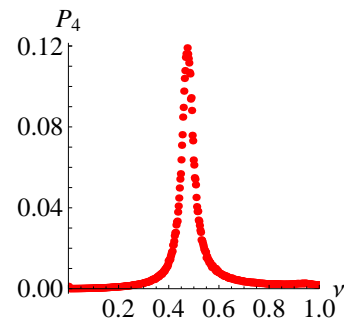


FIG. 3: (Color online) Power spectrum for the fluctuations of infectives from simulation of a three-city model with equal population sizes plotted as a function of the frequency  $\nu = \omega/(2\pi) 1/y$ . The spectrum shown corresponds to city 1, the spectra for the other cities are very similar. Metapopulation model parameters:  $N_1 = N_2 = N_3 = 10^6$ ,  $c_{12} = 0.06$ , and  $c_{13} = c_{23} = 0.02$ . Epidemiological parameters:  $\gamma = 365/13 1/y$ ,  $\mu = 1/50 1/y$ , and  $\beta = 17(\gamma + \mu)$ .

peak is present for a large range of parameter values. An example is shown in Fig. 3, where typical values for measles [7, 10, 34] were chosen for the epidemiological parameters (we shall keep these values fixed throughout this section).

To understand how this comes about, we first note that the number of peaks in the power spectrum is given by the form of the denominator,  $|\det \Phi(\omega)|^2$ ; the numerator essentially just shifts the position of these peaks somewhat. Therefore we can understand the number and nature of the peaks by studying the eigenvalues of  $\Phi_{JK}$ , which are those of the matrix  $A_{JK}$  shifted by  $-i\omega$ .

Each pair of complex conjugate eigenvalues of  $A_{JK}$ ,  $\lambda_c, \lambda_c^*$ , will give rise to a factor in  $|\det \Phi(\omega)|^2$  of the form  $(|\lambda_c|^2 - \omega^2)^2 + [2 \operatorname{Re}(\lambda_c)\omega]^2$ , and each real eigenvalue of  $A_{JK}$ ,  $\lambda_r$ , yields a factor of the form  $(\lambda_r^2 + \omega^2)^2$ . Peaks in the power spectrum are associated with complex eigenvalues  $\lambda_c$  of  $A_{JK}$  with small real parts, and their position is approximately given by  $\omega \approx \operatorname{Im}(\lambda_c)$ . In the trivial case of one city,  $n = 1$ ,  $A_{JK}$  has a pair of complex conjugate eigenvalues  $\lambda_1^\pm$  with  $\operatorname{Re}(\lambda_1^\pm) = -\beta\mu/(2(\gamma + \mu))$  and  $|\lambda_1^\pm| = \sqrt{\mu(\beta - \gamma - \mu)}$  (see Appendix B). The conditions for a pronounced peak for  $\omega$  close to  $\operatorname{Im}(\lambda_1^\pm) \approx |\lambda_1^\pm|$  are fulfilled because  $\mu$ , the death-birth rate, is small. This carries over to the general  $n$  city case since, as shown in Appendix B,  $\lambda_1^\pm$  always belong to the set of eigenvalues of  $A_{JK}$ . For the parameter values of Fig. 3 the numerical values of the common eigenvalue pair are  $\lambda_1^\pm = -0.17 \pm i 2.99$ , so we expect a peak to be located close to  $\nu = \operatorname{Im}(\lambda_1^\pm)/(2\pi) \approx 0.48 1/y$ .

For large demographic coupling, the  $n$  city system will behave as well mixed system comprising all the cities and we expect to find in that limit a power spectrum similar to the case  $n = 1$ , where each city contributes proportionally to its size to the overall spectral density. In the opposite limit, the  $n$  cities uncouple and we will find for each city the power spectrum of the one city case. In or-

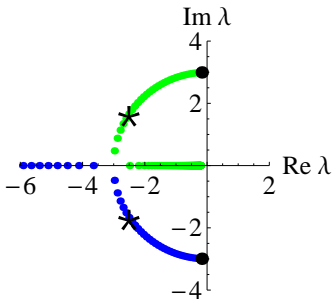


FIG. 4: (Color online) An Argand diagram of the eigenvalues for the two-city model with  $q = N_2/N_1 = 3/2$  and  $c_{12} \in [0, 1]$ . The large black dots are the common eigenvalue pair  $\lambda_1^\pm$ . The sets of smaller dark gray (blue) and light gray (green) dots are the remaining eigenvalues  $\lambda_2^\pm$  computed on a uniform grid of values of  $c_{12}$  in the interval. The eigenvalues with  $\text{Re } \lambda_2^- < -6$  are not shown in the plot, they are found for  $c_{12} > 0.15$ . The asterisks show the eigenvalues for the parameter values used in Fig. 5.

der to understand why additional peaks do not show up in simulations for intermediate coupling strengths, it is useful to consider the case  $n = 2$ , for which the eigenvalues of  $A_{JK}$  can be determined analytically and depend on a single coupling parameter  $c_{12}$  and the ratio of the population sizes  $q = N_2/N_1$  (see Eq. (6) and Appendix B). An Argand diagram of the two pairs of eigenvalues,  $\lambda_1^\pm$  and  $\lambda_2^\pm$ , for the two-city model is shown in Fig. 4. It can be seen that as the coupling increases,  $\lambda_2^\pm$  follow the circle  $\mathcal{C}$  centered at zero that goes through  $\lambda_1^\pm$ , moving away from the imaginary axis. Real and imaginary parts become of the same order for very small values of the coupling, and so we expect the power spectrum to be always dominated by the peak associated with  $\lambda_1^\pm$  that characterizes the spectrum in the uncoupled case. This behavior carries over to the  $n$ -city case with symmetric coupling, for which a complete analysis of the eigenvalues of  $A_{JK}$  can also be given, see Appendix B. In particular, it can be shown that apart from the common eigenvalue pair  $\lambda_1^\pm$   $A_{JK}$ , has a single  $(n - 1)$ -fold degenerate additional eigenvalue pair that behaves as a function of the coupling parameter as described above for  $n = 2$ .

For the coupling parameter that corresponds to the values of  $\lambda_2^\pm$  marked with asterisks in Fig. 4 and for a certain choice of population sizes, the infective fluctuations power spectra for the two-city model obtained from simulations and from Eq. (25) are shown in Fig. 5. We find a nearly perfect match between the results of numerical simulations and the analytical calculations. In agreement with the above argument the power spectra of city 1 and city 2 are very similar to the power spectrum of the one city case, which in turn is very similar to the spectrum shown in Fig. 3 for 3 cities with small coupling. In all cases the functional form of the spectral density is dominated by the peak associated with the common eigenvalue pair  $\lambda_1^\pm$ . As for the amplitudes of the power spectra  $P_J(\nu)$ , their ratio with respect to the

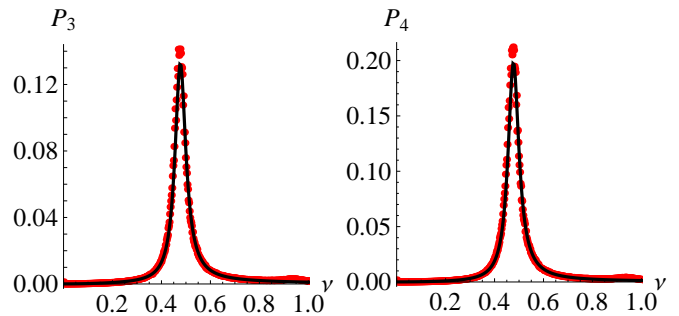


FIG. 5: (Color online) Power spectra for the fluctuations of infectives from simulation of the two-city model [(red) dots] and analytic calculation (black solid curve) plotted as a function of the frequency  $\nu = \omega/(2\pi) 1/y$ . The population sizes were chosen to be  $N_1 = 10^6$  and  $N_2 = 1.5 \times 10^6$  so that their ratio is  $3/2$ . The coupling coefficient  $c_{12} = 0.1$ . The location of the eigenvalues for this choice of parameters is indicated in Fig. 4 by asterisks and large dots.

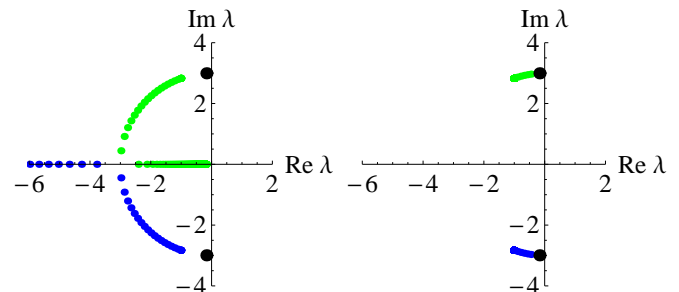


FIG. 6: (Color online) An Argand diagram of the eigenvalues for a three-city model with equal population sizes,  $c_{12} \in [0, 0.98]$  and the other parameters as in Fig. 3. The large black dots are the common eigenvalue pair  $\lambda_1^\pm$ . The sets of smaller dark gray (blue) and light gray (green) dots are the remaining eigenvalues  $\lambda_2^\pm$  (left panel) and  $\lambda_3^\pm$  (right panel) computed on a uniform grid of values of  $c_{12}$  in the interval. The eigenvalues with  $\text{Re } \lambda_2^- < -6$  are not shown in the plot, they are found for  $c_{12} > 0.12$ .

one city case,  $r_J(\nu)$ , decreases as the coupling increases. For two cities and  $q = 1$ , the power spectra  $P_3$  and  $P_4$  of city 1 and city 2 are equal and the relative peak amplitudes  $r_{3,4}(\nu_{\max})$  decrease with the coupling strength  $c_{12}$  down to 0.5. For other values of  $q$ , as in Fig. 5, the different peak amplitudes in two cities reflect the symmetry  $P_3(\nu; c_{12}, q) = P_4(\nu; c_{12}/q, 1/q)$ . Depending on  $q$ , the ratio  $r_{3,4}(\nu)$  may become even smaller than 0.5, but due to the symmetry that relates  $P_3$  and  $P_4$ , the amplitude of at least one of these peaks is always comparable to that of the uncoupled case. More precisely, it is easy to check that  $1 \leq r_3(\nu; c_{12}, q) + r_4(\nu; c_{12}, q) \leq 2$ , where the second inequality is satisfied strictly for  $c_{12} = 0$  and the lower bound corresponds to the large coupling limit  $c_{12} = 1$  and to  $\nu = \nu_{\max}$ .

The general case of three cities with no symmetry can also in principle be treated analytically because finding

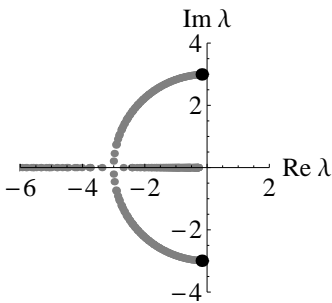


FIG. 7: An Argand diagram of the eigenvalues for a four-city model with the coupling strength  $x \in [0, 0.52]$ . The large black dots are the common eigenvalue pair  $\lambda_1^\pm$ . The remaining eigenvalues  $\lambda_{2,3,4}^\pm$  computed on a uniform grid of values of  $x$  in the interval are shown as sets of smaller gray dots. As in the previous figures we only show eigenvalues whose real part is larger than  $-6$ . Metapopulation model parameters:  $N_2/N_1 : N_3/N_1 : N_4/N_1 = 2 : 3 : 4$ ,  $\hat{c}_{12} = 1/\sqrt{\mu} = 2\hat{c}_{13} = 5\hat{c}_{14}/2 = 5\hat{c}_{23}/2 = 3\hat{c}_{24} = 4\hat{c}_{34}$ .

the eigenvalues of  $A_{JK}$  reduces to finding the roots of a fourth order polynomial. However, the problem now depends on 3 independent coupling parameters and 2 parameters for city sizes and closed form expressions are too lengthy to be useful. An approximate, concise description of the behavior of the eigenvalues of  $A_{JK}$  can be given in terms of only two parameters that measure coupling strength and coupling asymmetry, see Appendix B. In this approximation, we assume that all the  $c_{jk}$ ,  $j \neq k$ , are of order  $\sqrt{\mu}$  and treat  $\mu$  as the small parameter of the system. Simple expressions for the real parts and the absolute values of the additional eigenvalue pairs  $\lambda_2^\pm$ ,  $\lambda_3^\pm$  of  $A_{JK}$  up to terms of order  $\mu$  can be derived [see Eqs. (B22) and (B24)]. These show that, in this approximation, both eigenvalue pairs behave as described for the symmetric case. As the coupling increases, both eigenvalue pairs follow the circle  $\mathcal{C}$  centered at zero that goes through  $\lambda_1^\pm$ , moving away from the imaginary axis. The real and imaginary parts become of the same order within the scope of the approximation. Equation (B22) also shows how the asymmetry lifts the degeneracy of the two pairs  $\lambda_2^\pm$ ,  $\lambda_3^\pm$ . As the coupling increases, the two eigenvalue pairs move along the circle  $\mathcal{C}$  at different speeds. We have checked that Eqs. (B22) and (B24) give a good approximation to the exact results in the regime when the eigenvalues are complex.

The same behavior is illustrated in Fig. 6, where a plot of the exact solutions for  $\lambda_{2,3}^\pm$  is shown for parameter values that correspond to taking those of Fig. 3 and allowing one of the coupling coefficients to span the whole admissible range. One of the eigenvalues is shown only up to  $c_{12} = 0.12$ , where its real part becomes smaller than  $-6$ .

In Fig. 7 we show numerical results for the behavior of the eigenvalues of  $A_{JK}$  in the case of 4 cities with different population sizes and a certain choice of the coupling coefficients  $c_{jk}$ ,  $j, k = 1, 2, 3, 4$ . We make use of the following notation for the diagonal and off diagonal cou-

pling coefficients (see Appendix B):  $c_{jj} = 1 - \hat{c}_{jj} x \sqrt{\mu}$  and  $c_{jk} = \hat{c}_{jk} x \sqrt{\mu}$ , respectively. We then calculate the set of three non-trivial eigenvalue pairs as the coupling strength  $x$  varies in a suitable interval, keeping the  $\hat{c}_{jk}$  fixed. These results suggest that the behavior of the eigenvalues of  $A_{JK}$  is essentially given by the description of the symmetric case, and that more general couplings break the degeneracy as in the case  $n = 3$ , with no effects in the contributions to the peaks in the power spectrum.

## V. DISCUSSION AND CONCLUSIONS

In this paper we have extended the analysis of a metapopulation model of epidemics into the stochastic domain. Frequently epidemic models involving a spatial component, such as the interaction between several cities, are studied purely deterministically [28, 29] or through computer simulations [6, 13, 27]. We have demonstrated how a stochastic metapopulation model can be studied analytically by using a relatively straightforward extension of the methodology which was used to study a well-mixed population in a single city.

We adopted a simple specification of residents and commuters in order to set up the model. However, the coefficients which appear in the dynamical equations are generic and would appear in the same form if residents and commuters were included in a different way. It is evident that there are many ways of characterizing the interchange of individuals between cities which will result in the same model; only the identification of the coefficients with the underlying structure will be different.

The deterministic form of the model predicts that the system will reach a stable fixed point where the proportion of infected, susceptible and recovered individuals is the same in every city. The stochastic version of the model also predicts a clean simple result: that the large sustained oscillations which replace the deterministic predictions of constant behavior, have a single frequency which is the same for every city. Moreover, for small, large and intermediate coupling between the cities, the form of the power spectrum of these fluctuations is closely approximated by the power spectrum of the single city system.

It is remarkable that such a simple result occurs in what is a quite complicated stochastic nonlinear metapopulation model. We hope to explore the range of validity of this result and its robustness to the addition of new features to the model in the future. In any case, we believe that the work presented here will give a firm foundation to possible future work, including comparisons with the data available on childhood diseases.

## Acknowledgments

Financial support from the Portuguese Foundation for Science and Technology (FCT) under Contract

No. POCTI/ISFL/2/261 is gratefully acknowledged. G.R. was also supported by FCT under Grant No. SFRH/BPD/69137/2010.

### Appendix A: System-size expansion

Here we give some of the key steps in the application of the system-size expansion to the model explored in this paper. The method has been extensively discussed in the literature [6, 15, 19–25], and so we confine ourselves to a brief outline and to displaying the most important intermediate results in the derivation. We will assume that we are carrying out the calculation for the  $n$ -city case discussed in Section III; the corresponding results for Section II can be obtained simply by setting  $n = 2$ .

The first point to mention is that there are apparently  $n$  expansion parameters:  $\{N_1, \dots, N_n\}$ . The method is valid if they are all large and of the same order. More formally we can take, for instance,  $N_1 \equiv N$  as the expansion parameter and express all the other  $N_j$  in terms of it:  $N_j = Nq_j$ , where the  $q_j = N_j/N$ ,  $j = 2, \dots, n$  are of order one. In practice the method seems to work well when the  $q_j$  are significantly different from one, but this has to be checked a posteriori, for instance by comparing the analytic results with those obtained using computer simulations. In what follows we will not introduce the  $q_j$  explicitly; we will simply take all the  $N_j$ 's to be of the same order in the expansion.

The van Kampen ansatz Eq. (8) replaces the discrete stochastic variables  $\sigma$  by the continuous stochastic variables  $\mathbf{z}$  and so we write the transformed probability distribution  $P(\sigma, t)$  as  $\Pi(\mathbf{z}, t)$ . Since this transformation is time-dependent, substituting the ansatz into  $dP/dt$  on the left-hand side of Eq. (7) gives [15]

$$\begin{aligned} \frac{dP(\sigma, t)}{dt} &= \frac{\partial \Pi(\mathbf{z}, t)}{\partial t} - \sum_{j=1}^n \sqrt{N_j} \frac{\partial \Pi(\mathbf{z}, t)}{\partial x_j} \frac{ds_j}{dt} \\ &\quad - \sum_{j=1}^n \sqrt{N_j} \frac{\partial \Pi(\mathbf{z}, t)}{\partial y_j} \frac{di_j}{dt}. \end{aligned} \quad (\text{A1})$$

The right-hand side of the master equation (7) can be put into a form from which it is simple to apply the expansion procedure. To do this one introduces step-operators [15] defined by

$$\begin{aligned} \epsilon_{S_j}^{\pm 1} f(S_1, \dots, S_j, \dots, S_n, I_1, \dots, I_n) \\ &= f(S_1, \dots, S_j \pm 1, \dots, S_n, I_1, \dots, I_n), \\ \epsilon_{I_j}^{\pm 1} f(S_1, \dots, S_n, I_1, \dots, I_j, \dots, I_n) \\ &= f(S_1, \dots, S_n, I_1, \dots, I_j \pm 1, \dots, I_n), \end{aligned} \quad (\text{A2})$$

for a general function  $f$  and where  $j = 1, \dots, n$ . Using these operators the master equation (7) may be written

as

$$\begin{aligned} \frac{dP(\sigma, t)}{dt} &= \sum_{j=1}^n \left[ (\epsilon_{I_j} - 1) T_j + \left( \frac{\epsilon_{I_j}}{\epsilon_{S_j}} - 1 \right) T_{n+j} \right. \\ &\quad \left. + \left( \frac{1}{\epsilon_{S_j}} - 1 \right) T_{2n+j} + \left( \frac{\epsilon_{S_j}}{\epsilon_{I_j}} - 1 \right) T_{3n+j} \right] P(\sigma, t). \end{aligned} \quad (\text{A3})$$

Within the system-size expansion these operators have a simple structure:

$$\epsilon_{S_j} = \sum_{p=0}^{\infty} \frac{N_j^{-p/2}}{p!} \frac{\partial^p}{\partial x_j^p}, \quad \epsilon_{I_j} = \sum_{p=0}^{\infty} \frac{N_j^{-p/2}}{p!} \frac{\partial^p}{\partial y_j^p}, \quad (\text{A4})$$

and so all the terms of the right-hand side of Eq. (A3) may be straightforwardly expanded. Comparing these with the left-hand side in Eq. (A1) the leading order ( $\sim \sqrt{N_j}$ ) yields the deterministic equations given by Eq. (18). The next-to-leading order (which is of order one) gives a Fokker-Planck equation:

$$\frac{\partial \Pi}{\partial t} = - \sum_{J,K=1}^{2n} \frac{\partial}{\partial z_J} [A_{JK} z_K \Pi] + \frac{1}{2} \sum_{J,K=1}^{2n} B_{JK} \frac{\partial^2 \Pi}{\partial z_J \partial z_K}. \quad (\text{A5})$$

The  $2n \times 2n$  matrices  $A$  and  $B$  which appear in this equation have the following form. Writing  $A$  in blocks of four  $n \times n$  submatrices:

$$A = \begin{bmatrix} A^{(1)} & A^{(2)} \\ A^{(3)} & A^{(4)} \end{bmatrix}, \quad (\text{A6})$$

the elements of these submatrices are

$$\begin{aligned} A_{jk}^{(1)} &= -\mu \delta_{jk} - \beta \delta_{jk} \sum_{\ell=1}^n c_{j\ell} i_{\ell}, \\ A_{jk}^{(2)} &= -\beta \left( \frac{N_j}{N_k} \right)^{1/2} s_j c_{jk}, \\ A_{jk}^{(3)} &= \beta \delta_{jk} \sum_{\ell=1}^n c_{j\ell} i_{\ell}, \\ A_{jk}^{(4)} &= -(\mu + \gamma) \delta_{jk} + \beta \left( \frac{N_j}{N_k} \right)^{1/2} s_j c_{jk}. \end{aligned} \quad (\text{A7})$$

Writing  $B$  in a similar way to  $A$  in Eq. (A6), the elements of the submatrices are

$$\begin{aligned} B_{jk}^{(1)} &= \mu \delta_{jk} (1 - s_j) + \beta \delta_{jk} \sum_{\ell=1}^n s_j c_{j\ell} i_{\ell}, \\ B_{jk}^{(2)} &= B_{jk}^{(3)} = -\mu \delta_{jk} i_j - \beta \delta_{jk} \sum_{\ell=1}^n s_j c_{j\ell} i_{\ell}, \\ B_{jk}^{(4)} &= (\gamma + \mu) \delta_{jk} i_j + \beta \delta_{jk} \sum_{\ell=1}^n s_j c_{j\ell} i_{\ell}. \end{aligned} \quad (\text{A8})$$

From Eqs. (A7) and (A8) it is clear that the matrices  $A_{jk}$  and  $B_{jk}$  depend on the solutions of the deterministic

equations given in Eq. (18). However, since we will be interested only in fluctuations about the stationary state, these matrices are evaluated at the fixed point. Since the unique stable fixed point is the symmetric one, the same for all cities, the entries (A7) and (A8) are given by:

$$\begin{aligned} A_{jk}^{*(1)} &= -[\mu + \beta i^*] \delta_{jk}, & A_{jk}^{*(2)} &= -\beta \left( \frac{N_j}{N_k} \right)^{1/2} s^* c_{jk}, \\ A_{jk}^{*(3)} &= \beta i^* \delta_{jk}, & A_{jk}^{*(4)} &= \beta \left( \frac{N_j}{N_k} \right)^{1/2} s^* c_{jk} - (\mu + \gamma) \delta_{jk}, \end{aligned} \quad (\text{A9})$$

and

$$\begin{aligned} B_{jk}^{*(1)} &= 2\mu(1 - s^*) \delta_{jk}, & B_{jk}^{*(4)} &= 2(\gamma + \mu) i^* \delta_{jk}, \\ B_{jk}^{*(2)} &= B_{jk}^{*(3)} = -i^* [\mu + \beta s^*] \delta_{jk}, \end{aligned} \quad (\text{A10})$$

where we have used the fixed-point equation (21) to simplify some of the entries in Eq. (A10).

Finally, the Fokker-Planck equation (A5) is equivalent to the stochastic differential equation (10). We will work with the latter, since we wish to use Fourier analysis to analyze the nature of the fluctuations, and since Eq. (10) is linear, it can easily be Fourier transformed, as discussed in detail in Section IV.

## Appendix B: Some results for the $n$ -city case

In this Appendix we give some of the derivations for the  $n$ -city case discussed in Section III and Section IV which are too long and cumbersome to be given in the main text.

### 1. The coefficients $c_{jk}$

The coefficients  $c_{jk}$  appearing in Eq. (16) may be read off from the four types of term (i)-(iv) given in Section III:

$$\begin{aligned} c_{jj} &= \frac{(1 - f_j)^2 N_j}{\left[ (1 - f_j) N_j + \sum_{m \neq j} f_{jm} N_m \right]} \\ &+ \sum_{\ell \neq j} \frac{f_{\ell j}^2 N_j}{\left[ (1 - f_\ell) N_\ell + \sum_{m \neq \ell} f_{\ell m} N_m \right]}, \end{aligned} \quad (\text{B1})$$

for  $j = 1, \dots, n$  and

$$\begin{aligned} c_{jk} &= \frac{(1 - f_j) f_{jk} N_k}{\left[ (1 - f_j) N_j + \sum_{m \neq j} f_{jm} N_m \right]} \\ &+ \frac{f_{kj} (1 - f_k) N_k}{\left[ (1 - f_k) N_k + \sum_{m \neq k} f_{km} N_m \right]} \\ &+ \sum_{\ell \neq j, k} \frac{f_{\ell j} f_{\ell k} N_k}{\left[ (1 - f_\ell) N_\ell + \sum_{m \neq \ell} f_{\ell m} N_m \right]}, \end{aligned} \quad (\text{B2})$$

for  $j, k = 1, \dots, n$  and  $j \neq k$ .

To prove the first relation given in Eq. (17), consider the sum  $c_{jj} + \sum_{k \neq j} c_{jk}$ . The first term in Eq. (B1) combines with the first term in Eq. (B2) to give  $(1 - f_j)$ . The last term in Eq. (B1) combines with the last term in Eq. (B2) to give

$$\begin{aligned} &\sum_{\ell \neq j} \frac{f_{\ell j} \left[ f_{\ell j} N_j + \sum_{k \neq j, \ell} f_{\ell k} N_k \right]}{\left[ (1 - f_\ell) N_\ell + \sum_{m \neq \ell} f_{\ell m} N_m \right]} \\ &= \sum_{\ell \neq j} \frac{f_{\ell j} \left[ \sum_{k \neq \ell} f_{\ell k} N_k \right]}{\left[ (1 - f_\ell) N_\ell + \sum_{m \neq \ell} f_{\ell m} N_m \right]} \\ &= \sum_{k \neq j} \frac{f_{kj} \left[ \sum_{m \neq k} f_{km} N_m \right]}{\left[ (1 - f_k) N_k + \sum_{m \neq k} f_{km} N_m \right]}, \end{aligned} \quad (\text{B3})$$

where in the last line we have performed a relabeling. Combining the middle term of Eq. (B2) with the result in Eq. (B3) gives

$$\sum_{k \neq j} \frac{f_{kj} \left[ (1 - f_k) N_k + \sum_{m \neq k} f_{km} N_m \right]}{\left[ (1 - f_k) N_k + \sum_{m \neq k} f_{km} N_m \right]} = f_j, \quad (\text{B4})$$

using Eq. (11). Adding this to the result  $(1 - f_j)$  found earlier proves the result  $c_{jj} + \sum_{k \neq j} c_{jk} = 1$ .

We also note from Eq. (B2) that  $c_{jk}/N_k$  is symmetric under the interchange of  $j$  and  $k$ . Therefore

$$\frac{c_{jk}}{N_k} = \frac{c_{kj}}{N_j}, \quad (\text{B5})$$

which is the second relation in Eq. (17).

### 2. Uniqueness and stability of the fixed point

In Section III we asserted that the deterministic equations (18) have a unique non-trivial fixed point, which was globally stable. Here we prove this by giving a Liapunov function for the dynamical system in the invariant region  $R = \{(s_1, \dots, s_n, i_1, \dots, i_n) : 0 \leq s_j \leq 1, 0 \leq i_j \leq 1, s_j + i_j \leq 1, j = 1, \dots, n\}$  where the system is defined. This is a modification of the function given in Ref. [33] for the SEIR model. The proof assumes that the matrix of the coupling coefficients  $c_{jk}$  is irreducible, which means that any two cities have a direct or indirect interaction. Otherwise the proof breaks down because the  $n$  cities may be split into non-interacting subsets, and several equilibria may be found by combining disease extinction in some subsets with non-trivial equilibrium in other subsets.

Let  $\beta_{jk} \equiv \beta c_{jk} s_j^* i_k^*$ , where  $(s_1^*, \dots, s_n^*, i_1^*, \dots, i_n^*)$  is a fixed point of Eq. (18), and denote by  $M$  the matrix defined by  $M_{kj} = \beta_{jk}$ ,  $j \neq k$ , and  $\sum_{k=1}^n M_{kj} = 0$ ,  $j = 1, \dots, n$ . It can be shown ([33], Lemma 2.1) that the solution space of the linear equation  $Mv = 0$  is spanned

by a single vector  $(v_1, \dots, v_n)$ ,  $v_j > 0, j = 1, \dots, n$ . Let  $L(s_1, \dots, s_n, i_1, \dots, i_n)$  be defined as

$$L = \sum_{j=1}^n v_j (s_j - s_j^* \log s_j + i_j - i_j^* \log i_j).$$

$L$  has a global minimum in  $R$  at the fixed point. Functions of this form have been used in the literature as Liapunov functions for fixed points of ecological and epidemiological models, whose variables take only positive values [33]. Differentiating  $L$  along the solutions of Eq. (18), and following the proof of Theorem 1.1 in Ref. [33], we obtain

$$\dot{L} \leq \sum_{j,k=1}^n v_j M_{kj} \left( 2 - \frac{s_j^*}{s_j} - \frac{s_j}{s_j^*} \frac{i_k}{i_k^*} \frac{i_j^*}{i_j} \right). \quad (\text{B6})$$

The properties of the coefficients  $v_j$  in the definition of  $L$  play a crucial role in the derivation of the second term in this inequality. Use has been made of the identity

$$\sum_{j=1}^n v_j \sum_{k=1}^n \beta c_{jk} s_j^* i_k = \sum_{j=1}^n v_j (\gamma + \mu) i_j, \quad (\text{B7})$$

which in turn uses the fact that  $Mv = 0$  can be written as

$$\sum_{j=1}^n \beta c_{kj} s_k^* i_j^* v_k = \sum_{j=1}^n \beta c_{jk} s_j^* i_k^* v_j, \quad , k = 1, \dots, n. \quad (\text{B8})$$

Following Ref. [33], it can then be shown that the right-hand side of Eq (B6) is strictly negative except at  $(s_1^*, \dots, s_n^*, i_1^*, \dots, i_n^*)$ . Therefore,  $L$  is a Liapunov function for this fixed point in  $R$ , and the fixed point is unique and globally stable. Note that the result also holds when the disease transmissibility  $\beta$ , the recovery rate  $\gamma$  and the birth-death rate  $\mu$  are different in different cities, in which case the non-trivial equilibrium is in general not symmetric.

### 3. Nature of the eigenvalues of the matrix $A$

In this subsection we will give some results on the eigenvalues of  $A$  which are required for the discussion in Section IV.

We first recall that  $A$  is closely related to the stability matrix of the deterministic equations (18). In fact, in most applications of the system-size expansion they are equal. In our case because we have  $n$  expansion parameters  $\sqrt{N_j}$ , they are not equal, but closely related. A simple calculation of the Jacobian,  $J$ , from Eq. (18), shows that

$$J = S^{-1}AS, \quad \text{where } S = \text{diag} \left( \sqrt{N_1}, \dots, \sqrt{N_n} \right). \quad (\text{B9})$$

The effect of the transformation is simply that one can obtain  $J$  from  $A$  by omitting the terms  $(N_j/N_k)^{1/2}$  in

$A_{jk}^{(2)}$  and  $A_{jk}^{(4)}$  in Eq. (A7) or in  $A_{jk}^{*(2)}$  and  $A_{jk}^{*(4)}$  in Eq. (A9). This is useful, since it follows from the similarity transformation (B9) that the eigenvalues of  $A$  are also the eigenvalues of  $J$ . So we may study the simpler problem of finding the eigenvalues of the Jacobian at the symmetric fixed point (22).

For orientation, let us explicitly calculate the characteristic polynomial of the Jacobian for the cases of one city and two cities. These are

$$n = 1 : \quad R_1(\lambda) = Q^{-1}(d_2\lambda^2 + d_1\lambda + d_0), \quad (\text{B10})$$

where

$$\begin{aligned} Q &= \gamma + \mu, \quad d_2 = \gamma + \mu, \quad d_1 = \beta\mu, \\ d_0 &= \mu(\gamma + \mu) [\beta - (\gamma + \mu)], \end{aligned} \quad (\text{B11})$$

and

$$n = 2 : \quad R_2(\lambda) = Q^{-2}(d_2\lambda^2 + d_1\lambda + d_0)(g_2\lambda^2 + g_1\lambda + g_0).$$

Thus,

$$R_2(\lambda) = R_1(\lambda)Q^{-1}(g_2\lambda^2 + g_1\lambda + g_0), \quad (\text{B12})$$

where

$$\begin{aligned} g_2 &= \gamma + \mu, \quad g_1 = \beta\mu + (c_{12} + c_{21})(\gamma + \mu)^2, \\ g_0 &= \mu(\gamma + \mu) [\beta - (1 - c_{12} - c_{21})(\gamma + \mu)]. \end{aligned} \quad (\text{B13})$$

We see that the factor  $R_1(\lambda)$  is common, which suggests that the pair of eigenvalues found in the one city case might always be present in the  $n$  city case. This is easily proved by considering the vector  $\mathbf{v} = (v_1, \dots, v_n, v_{n+1}, \dots, v_{2n})^T$  with components satisfying  $v_i = v$  and  $v_{i+n} = v'$  for  $i = 1, \dots, n$ . Then the eigenvector equation  $J^*\mathbf{v} = \lambda\mathbf{v}$  reduces to that for one city as required.

A similar method can be used to find the characteristic polynomial for  $n \geq 3$  cities with equal population sizes, where the couplings are equal, that is,

$$c_{jk} = \begin{cases} 1 - (n-1)c, & j = k, \\ c, & j \neq k, \end{cases} \quad (\text{B14})$$

where  $j, k = 1, \dots, n$ . We now take the components of the vector to be  $v_1 = -v_2 = v$ ,  $v_{n+1} = -v_{n+2} = v'$ , and  $v_i = v_{i+n} = 0$  for  $i = 3, \dots, n$ . The eigenvector equation  $J^*\mathbf{v} = \lambda\mathbf{v}$  now reduces to

$$\begin{aligned} - \left( \frac{\beta\mu}{\gamma + \mu} + \lambda \right) v - (1 - nc)(\gamma + \mu)v' &= 0, \\ \left( \frac{\beta\mu}{\gamma + \mu} - \mu \right) v - [nc(\gamma + \mu) + \lambda]v' &= 0. \end{aligned} \quad (\text{B15})$$

Therefore, both solutions of

$$Q^{-1} (h_2\lambda^2 + h_{1n}\lambda + h_{0n}) = 0, \quad (\text{B16})$$

where

$$\begin{aligned} h_2 &= \gamma + \mu, & h_{1n} &= \beta\mu + nc(\gamma + \mu)^2, \\ h_{0n} &= \mu(\gamma + \mu) [\beta - (1 - nc)(\gamma + \mu)], \end{aligned} \quad (\text{B17})$$

are eigenvalues of  $J^*$ . This procedure can be repeated for  $n - 1$  independent vectors with only four non-zero components and the same symmetry as  $\mathbf{v}$ . Therefore, the characteristic polynomial of  $J^*$ ,  $R_n(\lambda)$ , factorizes as

$$R_n(\lambda) = R_1(\lambda) [Q^{-1} (h_2\lambda^2 + h_{1n}\lambda + h_{0n})]^{n-1}. \quad (\text{B18})$$

Finally let us consider 3 cities with arbitrary coupling and study the eigenvalues of  $J^*$  in the limit when the off-diagonal coefficients  $c_{jk}$  are small and of the same order. It will become clear that the coupling range to explore corresponds to  $c_{jk}$  of the order of  $\sqrt{\mu}$  and it is convenient to introduce the notation

$$c_{jk}(x) = \begin{cases} 1 - \hat{c}_{jj} x \sqrt{\mu}, & j = k, \\ \hat{c}_{jk} x \sqrt{\mu}, & j \neq k, \end{cases} \quad (\text{B19})$$

where  $j, k = 1, 2, 3$  and  $x$  is a positive parameter. Eq. (B19) represents, for each choice of  $\hat{c}_{jk}$ , a family of systems with all the off-diagonal coefficients  $c_{jk}$  of the same order, that reaches the zero coupling limit for  $x = 0$ . The quantity  $x$  measures the distance to zero coupling along each particular family, scaled by  $\sqrt{\mu}$ . Taking into account the properties of the matrix  $c_{jk}$ , given by Eq. (17), the characteristic polynomial of  $J^*$  is a polynomial of degree six that can be expressed in terms of this distance  $x \sqrt{\mu}$  and of three other independent parameters. We choose these to be  $\hat{c}_{jj}$ ,  $j = 1, 2, 3$ . We know that this characteristic polynomial factorizes as  $R_1(\lambda)(\lambda^4 + p_3\lambda^3 + p_2\lambda^2 + p_1\lambda + p_0)$ , where  $p_3$ ,  $p_2$ ,  $p_1$  and  $p_0$  are some coefficients. The roots of  $R_1(\lambda)$  are the pair of eigenvalues  $\lambda_1^\pm$  shared by all the characteristic equations of this family of systems. The polynomial of degree four can be easily found by direct computation. For equal city sizes we obtain for the coefficients

$$\begin{aligned} p_3 &= \gamma\sigma x \sqrt{\mu} + \mathcal{O}(\mu), \\ p_2 &= 2(\beta - \gamma) \mu - 3/4 \gamma^2 \hat{p}_2 x^2 \mu + \mathcal{O}(\mu^{3/2}), \\ p_1 &= \gamma(\beta - \gamma)\sigma x \mu^{3/2} + \mathcal{O}(\mu^2), \\ p_0 &= (\beta - \gamma)^2 \mu^2 + \mathcal{O}(\mu^{5/2}), \end{aligned} \quad (\text{B20})$$

where

$$\begin{aligned} \sigma &= \hat{c}_{11} + \hat{c}_{22} + \hat{c}_{33}, \\ \hat{p}_2 &= \hat{c}_{11}^2 + \hat{c}_{22}^2 + \hat{c}_{33}^2 - 2(\hat{c}_{11}\hat{c}_{22} + \hat{c}_{11}\hat{c}_{33} + \hat{c}_{22}\hat{c}_{33}). \end{aligned} \quad (\text{B21})$$

Keeping only the leading order terms in each of the coefficients given by Eq. (B20) we find a simple approximate

expressions for the two additional eigenvalue pairs  $\lambda_2^\pm$ ,  $\lambda_3^\pm$ . In particular, we find

$$\begin{aligned} \text{Re}(\lambda_2^\pm) &= -\frac{\gamma}{4}(\sigma + k) x \sqrt{\mu} + \mathcal{O}(\mu), \\ \text{Re}(\lambda_3^\pm) &= -\frac{\gamma}{4}(\sigma - k) x \sqrt{\mu} + \mathcal{O}(\mu), \end{aligned} \quad (\text{B22})$$

where

$$k^2 = 4(\hat{c}_{11}^2 + \hat{c}_{22}^2 + \hat{c}_{33}^2 - \hat{c}_{11}\hat{c}_{22} - \hat{c}_{11}\hat{c}_{33} - \hat{c}_{22}\hat{c}_{33}). \quad (\text{B23})$$

Assuming without loss of generality that  $\hat{c}_{33} \geq \hat{c}_{22} \geq \hat{c}_{11}$ ,  $k^2$  is positive and so  $k$  is real. Note that  $k = 0$  in the symmetric case, and in that case (B22) coincide in the same order of approximation with the roots of Eq. (B16) for  $n = 3$ . The quantities  $\sigma x \sqrt{\mu}$  and  $k x \sqrt{\mu}$  that determine, in this approximation, the real parts of the two non-trivial eigenvalue pairs can be interpreted as the overall coupling strength and the coupling asymmetry for a system of family (B19). We also find for the absolute value of the eigenvalues

$$|\lambda_{2,3}^\pm| = \sqrt{\beta - \gamma} \sqrt{\mu} + \mathcal{O}(\mu), \quad (\text{B24})$$

which shows that, for all families of the form Eq. (B19), the eigenvalues  $\lambda_{2,3}^\pm$  of  $J^*$  move close to the circle  $\mathcal{C}$  in the complex plane centered at zero that goes through  $\lambda_1^\pm$ . For arbitrary city sizes, the same calculation can be carried out to find that Eq. (B22) and Eq. (B24) still hold, with Eq. (B23) replaced by

$$k^2 = \sigma^2 + \frac{1 + q_{21} + q_{31}}{q_{21}q_{31}} \tilde{k}^2, \quad (\text{B25})$$

where  $q_{jk} = N_j/N_k$  and

$$\tilde{k}^2 = \hat{c}_{11}^2 + (\hat{c}_{22}q_{21} - \hat{c}_{33}q_{31})^2 - 2\hat{c}_{11}(\hat{c}_{22}q_{21} + \hat{c}_{33}q_{31}). \quad (\text{B26})$$

The behavior of the two non-trivial eigenvalue pairs along a family (B19) can be described, in this approximation, in terms of the two parameters  $\sigma$  and  $k$  that characterize the family and of the scaled distance  $x$ . As  $x$  increases away from zero, both eigenvalue pairs move along  $\mathcal{C}$  with speeds whose ratio is given by  $(\sigma + k)/(\sigma - k)$ . The parameter  $k$  that measures the asymmetry of the coupling causes the splitting of the two pairs with respect to the degenerate, symmetric case. The first pair to reach the real axis does so for  $x = 4\sqrt{\beta - \gamma}/(\gamma(\sigma + k))$ , which lies within the scope of the approximation. From then on the two real eigenvalues keep changing with  $x$  in such a way that the square root of their product verifies the constraint Eq. (B24) until for large  $x$  the approximation breaks down.

- 
- [1] R. Pastor-Satorras and A. Vespignani, Phys. Rev. Lett. **86**, 3200 (2001).
- [2] M. J. Keeling and K. T. D. Eames, J. R. Soc. Interface **2**, 295 (2005).
- [3] T. Gross, C. J. D. D’Lima, and B. Blasius, Phys. Rev. Lett. **96**, 208701 (2006).
- [4] E. Volz and L. A. Meyers, Proc. R. Soc. B **274**, 2925 (2007).
- [5] V. Colizza, R. Pastor-Satorras, and A. Vespignani, Nature Phys. **3**, 276 (2007).
- [6] M. Simoes, M. M. Telo da Gama, and A. Nunes, J. R. Soc. Interface **5**, 555 (2008).
- [7] R. M. Anderson and R. M. May, *Infectious Diseases of Humans: Dynamics and Control* (Oxford University Press, Oxford, 1991).
- [8] M. J. Keeling and P. Rohani, *Modelling Infectious Diseases in Humans and Animals* (Princeton University Press, Princeton, 2007).
- [9] D. Schenzle, Math. Med. Biol. **1**, 169 (1985).
- [10] M. J. Keeling and B. T. Grenfell, Proc. R. Soc. London, Ser. B **269**, 335 (2002).
- [11] S. Eubank, H. Guclu, V. S. A. Kumar, M. V. Marathe, A. Srinivasan, Z. Toroczka, and N. Wang, Nature **429**, 180 (2004).
- [12] L. A. Meyers, B. Pourbohloul, M. E. J. Newman, D. M. Skowronski, and R. C. Brunham, J. Theor. Biol. **232**, 71 (2005).
- [13] C. Christensen, I. Albert, B. Grenfell, and R. Albert, Physica A **389**, 2663 (2010).
- [14] D. M. Aleman, T. G. Wibisono, and B. Schwartz, Interfaces **41**, 301 (2011).
- [15] N. G. van Kampen, *Stochastic Processes in Physics and Chemistry* (Elsevier, Amsterdam, 2007).
- [16] H. Risken, *The Fokker-Planck Equation* (Springer, Berlin, 1989).
- [17] D. T. Gillespie, J. Comp. Phys. **22**, 403 (1976).
- [18] A. J. McKane and T. J. Newman, Phys. Rev. Lett. **94**, 218102 (2005).
- [19] D. Alonso, A. J. McKane, and M. Pascual, J. R. Soc. Interface **4**, 575 (2007).
- [20] G. Rozhnova and A. Nunes, Phys. Rev. E **82**, 041906 (2010).
- [21] A. J. Black and A. J. McKane, J. Theor. Biol. **267**, 85 (2010).
- [22] A. J. Black, A. J. McKane, A. Nunes, and A. Parisi, Phys. Rev. E **80**, 021922 (2009).
- [23] A. J. Black and A. J. McKane, J. R. Soc. Interface **7**, 1219 (2010).
- [24] G. Rozhnova and A. Nunes, Phys. Rev. E **79**, 041922 (2009).
- [25] G. Rozhnova and A. Nunes, Phys. Rev. E **80**, 051915 (2009).
- [26] A. Lajmanovich and J. A. Yorke, Math. Biosci. **28**, 221 (1976).
- [27] A. L. Lloyd and R. M. May, J. Theor. Biol. **179**, 1 (1996).
- [28] M. J. Keeling and P. Rohani, Ecol. Lett. **5**, 20 (2002).
- [29] J. Arino and P. van den Driessche, Math. Populat. Studies **10**, 175 (2003).
- [30] T. J. Hagenaars, C. A. Donnelly, and N. M. Ferguson, J. Theor. Biol. **229**, 349 (2004).
- [31] V. Colizza and A. Vespignani, J. Theor. Biol. **251**, 450 (2008).
- [32] M. Barthelemy, C. Godreche, and J.-M. Luck, J. Theor. Biol. **267**, 554 (2010).
- [33] H. Guo, M. Y. Li, and Z. Shuai, Proc. Am. Math. Soc. **136**, 2793 (2008).
- [34] C. T. Bauch and D. J. D. Earn, Proc. R. Soc. London, Ser. B. **270**, 1573 (2003).